Available online at www.sciencedirect.com
SCIENCE DIRECT®
ELSEVIER
Mechanism and Machine Theory 39 (2004) 41–60
MECHANISM AND MACHINE THEORY
www.elsevier.com/locate/mechmt

Using CAD functionalities for the kinematics analysis of spatial parallel manipulators with 3-, 4-, 5-, 6-linearly driven limbs

Yi Lu *

Robotics Research Center, Department of Mechanical Engineering, Yanshan University, Qinhuangdao, Hebei 066004, PR China

Abstract

A novel computer aided geometric approach is put forward for designing the computer simulation mechanisms of spatial parallel manipulators with 3-, 4-, 5-, 6-driving limbs. Several new spatial parallel manipulators with 3-, 4-, 5-, 6-driving limbs are synthesized. Some common computer aided geometry constraints and dimension driving techniques and definitions for designing the simulation mechanisms are presented. Based on some new and original spatial parallel manipulators with 3-, 4-, 5-, 6-driving limbs, the 12 types of simulation mechanisms are created, respectively, by applying these techniques. When the driving dimensions of driving limbs are modified by using the dimension driving technique, the configurations of the simulation mechanisms are varied correspondingly, and the kinematic parameters of the moving platform are solved. The results of computer simulation prove that the computer aided geometric approach is not only fairly quick and straightforward, but is also advantageous from viewpoint of accuracy and repeatability.

Keywords: Computer aided geometry; Spatial parallel manipulator; Simulation mechanism

1. Introduction

Some spatial parallel manipulators with 3- or 6-driving limbs [1,2] have been utilized for many practical applications, in which the good kinematic and dynamic performance are adopted for the robot manipulator, the parallel machine tool, and the legs of walking machine, high load carrying capacity is used for the flight simulator, the automobile or tank simulator, the earthquake

* Tel.: +86-35-8057070; fax: +86-335-8061449.
E-mail address: luyip0736@sina.com (Y. Lu).

0094-114X/$ - see front matter
doi:10.1016/S0094-114X(03)00103-4

simulator, and so on [4–6]. Tsai [3] proved that in general, the number of driving limbs of the spatial parallel manipulator equals to the number of its DOF. In conducting the synthesis, kinematic analysis, and optimum design of the spatial parallel manipulators, some analytic approaches (such as the influence coefficient matrix approach [7], the screw approach [8], and the spatial vector analytic approach [9,10]) have been applied for studying the kinematic and dynamic performances of the spatial parallel manipulators with 3- or 6-driving limbs [7–17]. Up to now, the spatial parallel manipulators with 4- or 5-driving limbs have not been used for many practical applications, since the studies on them have not been perfect and mature.

The analytic approaches are suitable for computer programming and have the advantages of accuracy and repeatability. However, the calculation in the analytic processes of the spatial parallel mechanism is quite complicated, such as conducting the dimension synthesis, analyzing the kinematic and dynamics, and determining the singularity configuration. In terms of CAD mechanism analyses, based on the analytic approaches, some suitable programs are studied and compiled [18,19]. Since these analytic approaches are complex, the programming processes are complicated and not straightforward, especially in the case of multiple-solutions and the spatial parallel mechanisms. Therefore, the application of analytic approaches is limited. Currently, the computer aided geometric technology is an effective tool for feature designing, concept designing, 3D modeling, and synthesis and analysis of planar mechanism [20–25]. However, how to use this tool to solve kinematic and the SC analyses problems for spatial parallel manipulators with 3-, 4-, 5-, 6-driving limbs is still a key question, which has not been solved.

In order to solve the above problems, some simulation mechanisms of the spatial parallel manipulators with 3-, 4-, 5-, 6-driving limbs are designed, respectively, by using a CAD software with the functions of geometric constraint, equation constraint, and dimension driving functions. A novel computer aided geometric approach without modeling and assembling of 3D solid is explored for dynamically solving kinematic parameters.

2. The common technique for creating the simulation mechanisms

Before creating the simulation mechanisms of spatial parallel manipulators, some common techniques and definitions are described below.

Step 1. The dimensions in the simulation mechanisms are classified into the *driving dimension*, the *driven dimension*, and the *fixed dimension*. The driving dimensions are given to the driving limbs for driving the moving platform. The driven dimensions are given to the position and orientation of the moving platform in the respect to the base in order to solve kinematic parameters of mechanism. The fixed dimensions are given to the sideline of the moving platform, the sideline of the base, and the line for connecting any two joints in order to modify the size and configuration of the simulation mechanism.

Step 2. Some basic equivalent links in simulation mechanism are constituted as follows:

(a) Constitute a line l, and give it an initial fixed dimension. Thus, a line with fixed dimensions equivalent to a *binary link*.

(b) In 2D sketch environment of advanced CAD software, constitute an equilateral triangle, an equilateral quadrangle, and an equilateral hexagon, respectively, by using the polygon command. Transform them into an equilateral triangle plane, an equilateral quadrangle plane, and an equilateral hexagon plane, respectively, by using the planar area command. Give one sideline of polygon plane an initial fixed dimension by using dimension command. Thus, these polygon planes can be used as either the base or the moving platform, but they cannot be used as both, because the base and the moving platform cannot be constituted in 2D sketch environment at the same time. Therefore, if the base is constituted in 2D sketch environment, the moving platform must be constituted in 3D sketch environment by adopting steps 2c, 2d and 2e below, and vice versa.

(c) Constitute three lines l_i $(i = 1, 2, 3)$, and connect them to form a closed triangle $\Delta a_1a_2a_3$ by adopting the point–point coincident command. Next, give each sideline l_i of $\Delta a_1a_2a_3$ an initial driving dimension. Constitute a line c_1 connect its two ends to point a_1 and sideline l_3 by adopting the point–point coincident command and the point–line coincident command, respectively. Constitute a line c_2 and connect its two ends to point a_2 and line c_1 at point a_0. Set c_1 perpendicular to l_3 and set c_2 perpendicular to l_1 In this way, an equivalent planar ternary link in 3D sketch environment is constituted, and its center point a_0 is determined, as shown in Fig. 1a.

(d) Constitute four lines l_i $(i = 1, 2, 3, 4)$, and connect them to form a closed quadrangle $(a_1a_2a_3a_4)$ by using point–point coincident command. Set l_1 perpendicular to both l_2 and l_4 and set l_1 parallel to l_3. Thus, the four points (a_1, a_2, a_3, a_4) are always retained onto the same plane. Constitute a line c_1 and connect its two ends to a_1 and a_3, respectively. Constitute a line c_2 and connect its two ends to a_2 and a_4, respectively. Set c_1 perpendicular to c_2. Give one sideline of the quadrangle an initial dimension by using dimension command. In this way, an equivalent planar quadrangle link $(a_1a_2a_3a_4)$ in 3D sketch environment is constituted, and the central point a_0 of the link can be determined from the crossover point of c_1 and c_2 as shown in Fig. 1b.

(e) Constitute six lines l_i $(i = 1, 2, \ldots, 6)$, and connect them to form a closed hexagon $(a_1a_2a_3a_4a_5a_6)$ by adopting the point–point coincident command. Constitute a line c_1 and connect its two ends to a_3 and a_6, respectively. Constitute a line c_2 connect its two ends to a_1 and line c_1 at a_0, respectively, by using the point–point and point–line constraint command. Set c_1 parallel to both l_2 and l_5 and set c_2 parallel to both l_3 and l_6. Give same dimension to line c_2 and each of the sideline l_i. Thus, the six points a_i $(i = 1, 2, \ldots, 6)$ are always retained on the plane $\Delta a_1a_6a_0$. In this way, an equilateral hexagon plane $(a_1a_2a_3a_4a_5a_6)$ in 3D sketch environment is constituted, and its central point a_0 can be determined from the crossover point of c_1 and c_2 as shown in Fig. 1c.

Step 3. Some basic equivalent joints in simulation mechanism are constituted as follows:

(a) Constitute a line l, and give it a driving dimension in length. Thus, l is equivalent to a *prismatic joint p* or a driving limb with a prismatic joint P.

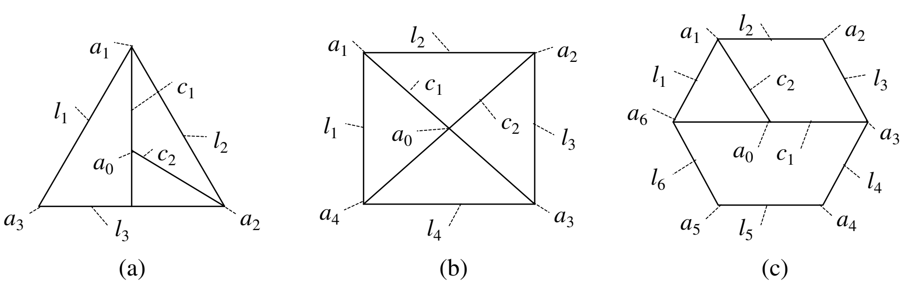

Fig. 1. (a) Equilateral ternary link; (b) equilateral quadrangle link and (c) equilateral hexagon link. The equivalent planar equilateral ternary, quadrangle, and hexagon links.

(b) Follow the step 2 above, constitute a link and a line l, connect one end of l to any point p on the link (such as the base, the moving platform, or another line) by using the point–point coincident command. Thus, the connecting point p is equivalent to a *spherical joint S*.

(c) Follow the step 2 above, constitute a link and a line l, connect one end of l to any vertex p on the link (such as the base, or the moving platform) or the end of another line by using the point–point coincident command, and set l perpendicular to another line on this link. Thus, the connecting point p is equivalent to a *revolving joint R*.

(d) Constitute two lines l_1 and l_2 connect one end of l_1 onto l_2 at point p by using the point–line coincident command, and set l_1 perpendicular to l_2. Thus, the connecting point p is equivalent to a *cylinder joint C*.

(e) Constitute two lines l_1 and l_2 connect one end of l_1 onto l_2 at point p by using the point–line coincident command, as shown in Fig. 2a. Thus, the connecting point p is equivalent to a *composite joint PS*.

Step 4. Follow the step 2 above, constitute a base B and a moving platform m, respectively. Follow the steps 3a and 3b above, constitute a line r_1 give r_1 a driving dimension in length, and connect its two ends to B at point A_1 and m at point a_1 respectively, by using the point–point coincident command. Thus, the two equivalent spherical joints S at point A_1 and point a_1 are constituted, respectively, and one equivalent *SPS driving limb* r_1 for connecting m and B is also constituted.

Step 5. Follow the step 4 above, set the driving limb r_1 perpendicular to one sideline of the base B. Thus, an equivalent revolving joint R for connecting r_1 and B is constituted. In this way, one equivalent SPS driving limb r_1 is transformed into an equivalent *SPR driving limb* r_1.

Step 6. Follow the step 4 above, constitute an auxiliary line B_1 and connect its one end to the base B at point A_1. Set B_1 perpendicular to both driving limb r_1 and a sideline of B (L_3 for the situation of the 3-driving limbs, and C_1 for the 4 driving limbs) by using perpendicular constraint command. Thus, one equivalent universal joint U at point A_1 on B is constituted. Similarly, constitute an auxiliary line b_1 connect its one end to m at point a_1 and set b_1 perpendicular to both r_1 and a sideline of m (l_3 for the 3-driving limbs, and c_1 for the 4-driving limbs). Thus, one equivalent universal joint U at point a_1 is constituted. Next, set B_1 parallel or perpendicular to b_1. In this way, one equivalent SPS driving limb r_1 is transformed into one equivalent *UPU driving limb* r_1 as shown in Fig. 2b.

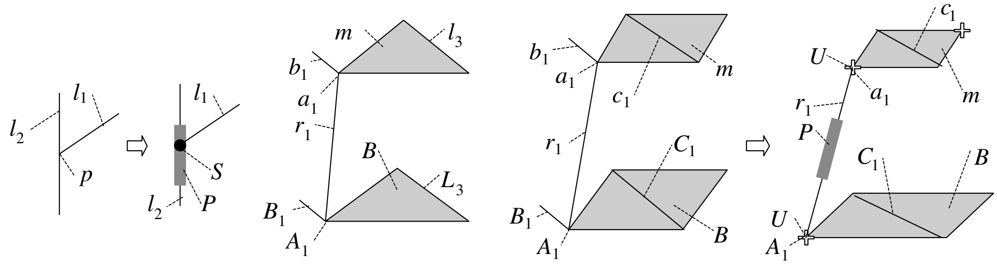

Fig. 2. (a) The equivalent a composite joint *PS* and (b) the equivalent UPU-driving limb r_1. The equivalent planar equilateral ternary, quadrangle, and hexagon links.

Step 7. Follow steps 4 and 6, constitute an equivalent spherical joint S at point A_1 on B and an equivalent universal joint U at point a_1 on m. In this way, one equivalent SPS driving limb r_1 is transformed into an equivalent *SPU driving limb* r_1. In fact, the SPU driving limb r_1 is equivalent to the SPS driving limb r_1 in simulation mechanism, because one local redundant DOF, which is produced from the driving limb rotating about itself axis, does not influence the motion of the moving platform. Therefore, the UPS driving limb r_1 in simulation mechanism can be replaced by the equivalent SPS driving limb r_1.

The DOF of the spatial parallel mechanism can be calculated by Kutzbach Grubler equation [2–4] below

$$F = \lambda(k - j - 1) + \sum_{i=1}^{n} f_i - F_0 \tag{1}$$

where k is the number of links, j is number of joints, λ is the degrees of the space within which the mechanism operates for spatial motions $\lambda = 6$; f_i is the degree of freedom of the ith joint, F_0 is the local redundant DOF, which do not influence the motion of mechanism.

3. The spatial parallel manipulator with 3-driving limbs

3.1. The 3-RPS parallel manipulator and its simulation mechanism

An existing spatial 3-RPS parallel manipulator has three DOF [2,3]. It includes a moving platform m, a base B, and three extendable driving limbs r_i with their hydraulic cylinders and piston-rods, as shown in Fig. 3a. Where, m is a regular triangle $\Delta a_1a_2a_3$ with a_0 as its center, and B

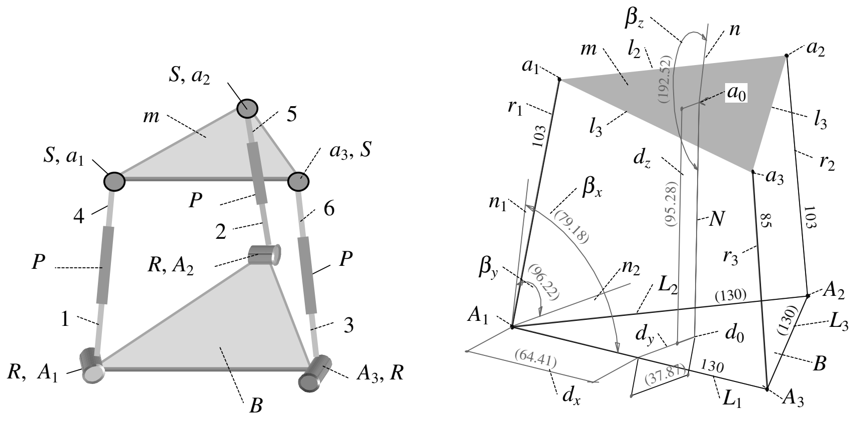

Fig. 3. (a) The spatial 3-SPR parallel manipulator and (b) its simulation mechanism. The spatial 3-SPR parallel manipulator and its simulation mechanism.

is a regular triangle $\Delta A_1A_2A_3$ with A_0 as its center. Three identical limbs connect m to B by a spherical joint S at point a_i, a driving limb with a prismatic joint P, and a revolute joint R at point A_i $(i = 1,2,3)$, respectively.

In the 3D sketch environment, a simulation mechanism of the 3-SPR spatial manipulator is created, as shown in Fig. 3b. The creation processes are explained as follows.

1. Follow the step 2 in the common technique, constitute the moving platform $\Delta a_1a_2a_3$ with a sideline (80 cm) in length, and the base $\Delta A_1A_2A_3$ with a sideline (130 cm) in length.
2. Follow step 5 in common technique, constitute an equivalent SPR driving limb r_1.
3. Repeat step 2 above, but (r_1 and L_3) are replaced by (r_2 and L_1) and (r_3 and L_2), respectively. Thus, the other two equivalent SPR driving limbs (r_2r_3) can be constituted. In this way, a 3-SPR parallel simulation mechanism is created.

3.2. The position-orientation of the moving platform

The position-orientation of the moving platform in the respect to the base of the 3-SPR simulation mechanism can be determined by following processes.

1. Constitute a line n, connect its one end to the center point a_0 on the moving platform m, and set line n perpendicular to m by adopting the perpendicular constraint command. In this way, a normal line n of m is constituted.
2. Constitute a line N, set it perpendicular to both sideline L_1 and sideline L_2 of the base B, and connect its one end to point a_0 on m by adopting the point–point coincident command.
3. Constitute a line d_y, connect its two ends to line N at point d_0 and sideline L_1, respectively, by adopting the point–line coincident command. Next, set d_y perpendicular to both N and L_1.
4. Give the distance from point a_0 to point d_0 an initial driven dimension d_z (95.28 cm), give the distance from point A_1 to line d_y an initial driven dimension d_x (64.41 cm), and give line d_y an initial driven dimension (37.87 cm) in length, respectively, by using dimension command. Thus, the three translation components (d_xd_y, d_z) of m are constituted, as shown in Fig. 3b.
5. Constitute line n_1 and line n_2 and connect their one ends to point A_1 on B, set n_1 parallel to n, and set n_2 perpendicular to both L_1 and N. Give the angle between n_1 and L_1 an initial driven dimension β_x (79.18°), give the angle between n_1 and n_2 an initial driven dimension β_y (96.22°), give the angle between n and N an initial driven dimension β_z (192.52°), respectively. Thus, the three rotation components $(\beta_x, \beta_y, \beta_z)$ of m are constituted, as shown in Fig. 3b.
6. When varying or modifying each driving dimension of the driving limb r_i, the driven dimensions of the three translation components (d_xd_y, d_z) and the three rotation components $(\beta_x, \beta_y, \beta_z)$ of m can be varied correspondingly. In this way, the position-orientation of the moving platform in respect to the base of the 3-SPR simulation mechanism can be solved dynamically.

3.3. The spatial 3-UPU parallel manipulator with 3-driving limbs

An existing spatial 3-UPU parallel manipulator has three DOF [3,4]. It includes a moving platform m, a base B, and three extendable driving limbs r_i with their hydraulic cylinders and

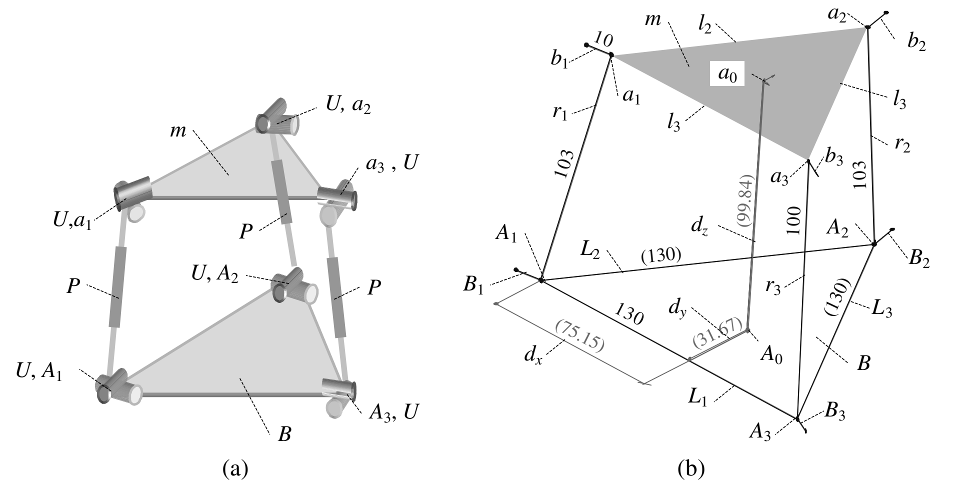

Fig. 4. (a) The spatial 3-UPU parallel manipulator and (b) its simulation mechanism. The spatial 3-UPU parallel manipulator and its simulation mechanism.

piston-rods as shown in Fig. 4a. Where, m is a regular triangle $\Delta a_1a_2a_3$ with a_0 as its center, and B is a regular triangle $A_1A_2A_3$ with A_0 as its center. Three identical UPU limbs connect m to B by a universal joint U at point a_i, a driving limb r_i with a prismatic joint P, and a universal joint U at point A_i for $i = 1$, 2, and 3, respectively.

In the 3D sketch environment, a simulation mechanism of the spatial 3-UPU manipulator is created, as shown in Fig. 4b. The creation processes are explained as follows.

1. Follow the step 2 in the common technique, constitute a moving platform $\Delta a_1a_2a_3$ with sideline (80 cm) in length, and a base $\Delta A_1A_2A_3$ with sideline (130 cm) in length, respectively.
2. Follow the step 6 in the common technique, constitute an equivalent UPU driving limb r_1. Similarly, replace (r_1 and L_3) by (r_2 and L_1) and (r_3 and L_2), respectively. Thus, the other two equivalent UPU driving limbs (r_2 and r_3) are constituted. In this way, a 3-UPU parallel simulation mechanism is created.
3. The position-orientation of the moving platform of the 3-UPU simulation mechanism can be solved by adopting similar processes in the Section 3.2.

3.4. The spatial 3-URPR parallel manipulator with 3-driving limbs

A new type of the spatial 3-URPR parallel manipulator is designed, as shown in Fig. 5a. It includes a moving platform m, a base B, three binary links, and three extendable driving limbs with their hydraulic cylinders and piston-rods. Where, m is a regular triangle $\Delta a_1a_2a_3$ with a_0 as its center, and B is a regular triangle $A_1A_2A_3$ with A_0 as its center. Three identical RPRU driving limbs connect m to B by a universal joint U at point a_i, a binary link g_i, a revolute joint R at point e_i, a driving rod r_i with a prismatic joint P, and a revolute joint R at point A_i $(i = 1, 2, 3)$, respectively.

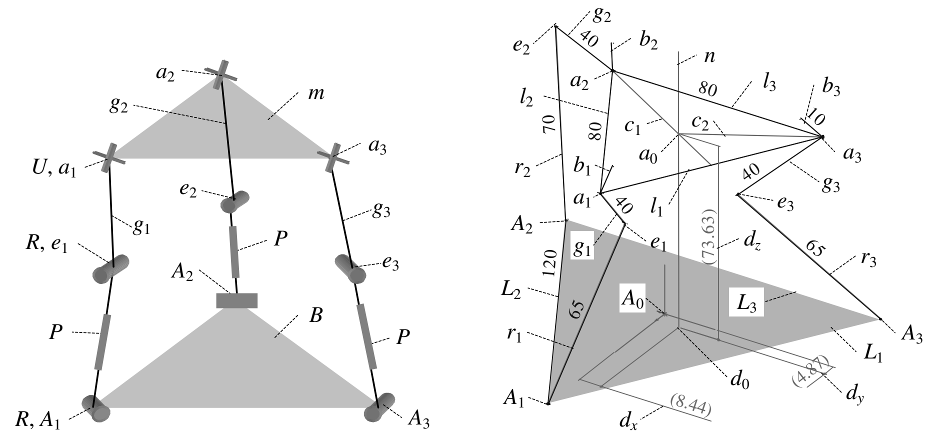

(a) (b)

Fig. 5. (a) The spatial 3-URPR parallel manipulator and (b) its simulation mechanism. The spatial 3-URPR parallel manipulator and its simulation mechanism.

By inspecting the whole 3-URPR parallel mechanism, we know that $k = 11$ for one moving platform, three binary links, three cylinders, and three piston-rods, and one base; $j = 12$ for three universal joints U, six revolute joints R, three prismatic joints P; $f_1 = 2$ for the universal joint, $f_2 = 1$ for the prismatic joint, $f_3 = 1$ for the revolute joint; $F_0 = 0$. Therefore, the DOF of the whole mechanism is

$$F = \lambda(k - j - 1) + \sum_{i=1}^{n} f_i - F_0 = 6 \times (11 - 12 - 1) + (3 \times 2 + 6 \times 1 + 3 \times 1) - 0 = 3 \qquad (2)$$

In the 3D sketch environment, a simulation mechanism of the spatial 3-URPR parallel manipulator is created, as shown in Fig. 5b. The creation processes are explained as follows.

1. Follow the step 2 in the common technique, constitute a moving platform $\Delta a_1a_2a_3$ with sideline (80 cm) in length, and a base $\Delta A_1A_2A_3$ with sideline (120 cm) in length, respectively.
2. Follow the step 3c in the common technique, set line r_1 perpendicular to line g_1 and set line r_1 perpendicular to a sideline L_3 of B. Thus, the two revolute joints R at point e_1 and point A_1 are constituted, respectively.
3. Follow the step 6 in the common technique, set an auxiliary line b_1 perpendicular to both l_1 and g_1 and set b_1 parallel to r_1. Thus, one equivalent universal joint U at point a_1 on m is constituted. In this way, an equivalent URPR driving limb is constituted.
4. Similarly, follow the steps 2 and 3 above, constitute the other two equivalent URPR driving limbs. In this way, a spatial 3-URPR simulation mechanism is created.
5. The position-orientation of the moving platform of the 3-URPR simulation mechanism can be determined by adopting the similar processes in Section 3.2.

From the 3-URPR simulation mechanism, we obtain two interesting conclusions:

(1) If the three lines g_i $(i = 1, 2, 3)$ are simultaneously reduced to 0 in length, then the spatial 3-URPR simulation mechanism is transformed into the spatial 3-SPR simulation mechanism.
(2) If the three lines g_i are exchanged with the 3-driving rods r_i $(i = 1, 2, 3)$ with a prismatic P, respectively, then the spatial 3-URPR simulation mechanism is transformed into a spatial 3-UPRR parallel manipulator and its DOF is not change. In this case, if the three lines g_i $(i = 1, 2, 3)$ are simultaneously reduced to 0 in length, then the spatial 3-UPRR simulation mechanism is transformed into a spatial 3-UPU simulation mechanism.

3.5. The spatial 3-SRP parallel manipulator with 3-driving limbs

A new type of spatial 3-SRP parallel manipulator is designed, as shown in Fig. 6a. It includes a moving platform m, a base B, three binary links, and three extendable driving limbs with their hydraulic cylinders and piston-rods, as shown in Fig. 5a. Where, m is a regular triangle $\Delta a_1a_2a_3$ with a_0 as its center, and B is a regular triangle $\Delta B_1B_2B_3$ with B_0 as its center. Three identical SRP driving limbs connect m to B by a spherical joint S at point a_i, a binary link g_i, a revolute joint R at point A_i and a driving limb r_i with a prismatic joint P, for $i = 1, 2$, and 3, respectively. The driving limb r_i with the prismatic joint P are retained coincident with the axis of revolute joint R_i and the sideline L_i of B $(i = 1, 2, 3)$, respectively.

By inspecting the whole mechanism of Fig. 6a, we know that $k = 8$ for one moving platform, three cylinders, and three piston-rods, and one base; $j = 9$ for three sphere joints S, three revolute joints R, and three prismatic joints P; $f_1 = 3$ for the sphere joint, $f_2 = 1$ for the prismatic joint,

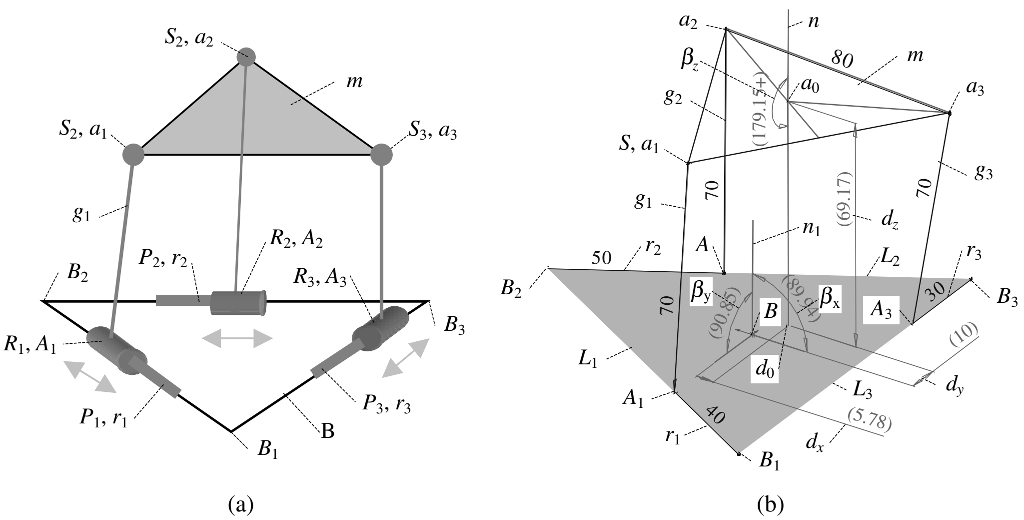

Fig. 6. (a) The spatial 3-SPR parallel manipulator and (b) its simulation mechanism. The spatial 3-SPR parallel manipulator and its simulation mechanism.

$f_3 = 1$ for the revolute joint; $F_0 = 0$. Therefore, based on Eq. (1), the DOF of the whole mechanism is

$$F = \lambda(k - j - 1) + \sum_{i=1}^{n} f_i - F_0 = 6 \times (8 - 9 - 1) + (3 \times 3 + 3 \times 1 + 3 \times 1) - 0 = 3 \tag{3}$$

In the 3D sketch environment, a simulation mechanism of the spatial 3-SPR manipulator is created, as shown in Fig. 6b. The creation processes are explained as follows.

1. Follow the step 2 in the common technique, constitute the moving platform $\Delta a_1a_2a_3$ with sideline (80 cm) in length, and the base $\Delta B_1B_2B_3$ with sideline (130 cm) in length, respectively.
2. Follow the step 4 in common technique, constitute a line g_1 connect its two ends to point a_1 on m and sideline L_1 at A_1 on B, and set g_1 perpendicular to L_1. Give the distance from point B_1 to point A_1 an initial driving dimension (40 cm). Thus, an equivalent SRP driving limb g_1r_1 is constituted.
3. Repeat the step 2 above, but (r_1, g_1 and L_1) are replaced by (r_2, g_2 and L_2) and (r_3, g_3 and L_3), respectively. Thus, other two equivalent SPR driving limbs (g_2r_2 and g_3r_3) are constituted. In this way, a 3-SRP parallel simulation mechanism is created.
4. The position-orientation of the moving platform of the 3-SRP simulation mechanism can be determined by adopting the similar processes in Section 3.2.

4. Spatial parallel manipulator with 4-driving limbs

A new type of spatial parallel mechanism with 4-driving limbs is designed, as shown in Fig. 7a. It includes a quaternary moving platform m, a quaternary base B, two extendable UPU limbs, and two extendable SPU limbs. Where, m is an equilateral quadrangle ($a_1a_2a_3a_4$) with a_0 as its center, and B is an equilateral quadrangle plane ($A_1A_2A_3A_4$) with A_0 as its center. Two identical SPU driving limbs connect m to B by a spherical joint S at point a_i, a driving limb r_i with a prismatic joint P, and a universal joint U at point A_i for $i = 2, 4$, respectively. Two identical UPU driving

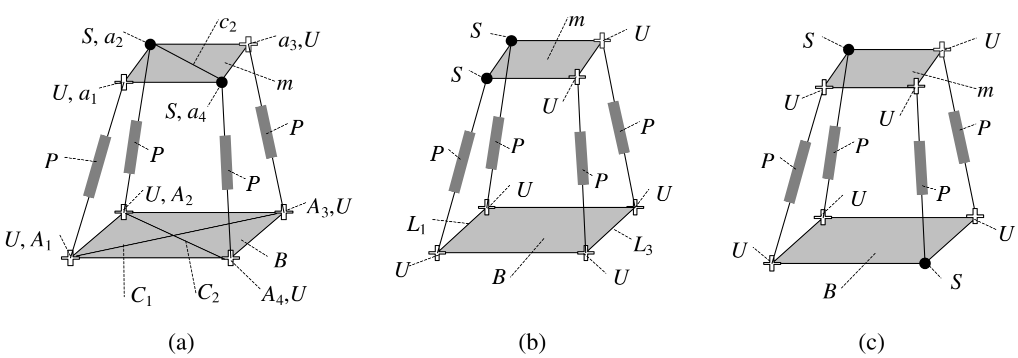

Fig. 7. (a) 2-SPU–UPU mechanism I; (b) 2-SPU–UPU mechanism II and (c) 2-SPU–UPU mechanism III. The spatial parallel mechanism with 4-driving limbs.

limbs connect m to B by a universal joint U at point a_i, a driving limb r_i with a prismatic joint P, and a universal joint U at point A_i for $i = 1, 3$, respectively. We define it as a 2-SPU–UPU mechanism I.

When 2-UPU limbs and 2-SPU limbs are arranged in different positions, the other two types of 2-SPU–UPU mechanism II and 2-SPU–UPU mechanism III can be synthesized, respectively, as shown in Fig. 7b and c.

By inspecting the whole mechanisms of Fig. 7, we know that $k = 10$ for one moving platform, four cylinders, and four piston-rods, and one base; $j = 12$ for six universal joints U, four prismatic joints P, and two sphere joints S; $f_1 = 2$ for the universal joint, $f_2 = 1$ for the prismatic joint, $f_3 = 3$ for the sphere joint; $F_0 = 0$. Therefore, based on Eq. (1), the DOF of the whole mechanism is

$$F = \lambda(k - j - 1) + \sum_{i=1'}^{n} f_i - F_0 = 6 \times (10 - 12 - 1) + (6 \times 2 + 4 \times 1 + 2 \times 3) - 0 = 4 \qquad (4)$$

A simulation mechanism I of the spatial 2-SPU–UPU parallel mechanism is created in the 3D sketch environment, as shown in Fig. 8a, and its creation processes are described below.

1. Follow the step 2 in the common technique, constitute a moving platform ($a_1a_2a_3a_4$) with sideline (60 cm) in length, and a base ($A_1A_2A_3A_4$) with sideline (100 cm) in length, respectively.
2. Follow the steps 6 and 7 in the common technique, constitute two equivalent UPU driving limbs (r_1 and r_3) and two equivalent SPU driving limbs (r_2 and r_4), respectively. In this way, a simulation mechanism of the spatial 2-SPU–UPU parallel mechanism I can be created.
3. The position-orientation of the moving platform of the 2-SPU–UPU simulation mechanism I can be determined by adopting similar processes in Section 3.2.

Similarly, a 2-SPU–UPU simulation mechanisms II is also created, as shown in Fig. 8b.

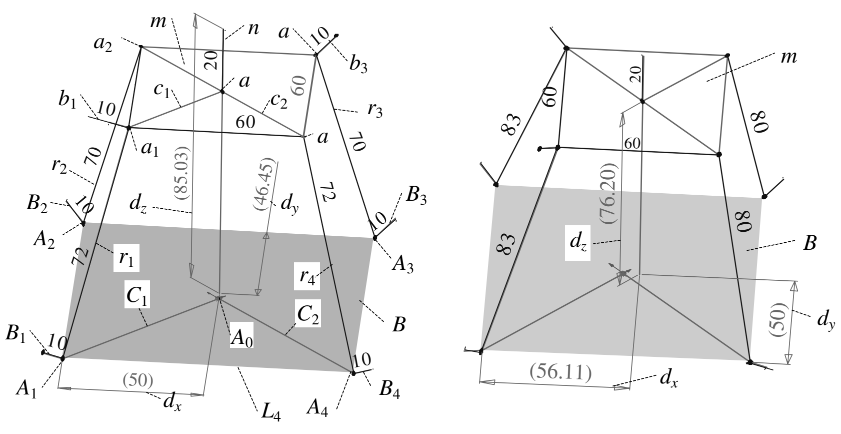

(a) (b)

Fig. 8. (a) The simulation mechanism I and (b) the simulation mechanism II. The simulation mechanisms of the 2-SPU–UPU parallel mechanism with 4-driving limbs.

5. Spatial parallel manipulator with 5-driving limbs

5.1. The 4-SPU and 1-UPU parallel manipulator and its simulation mechanism

A new type of the spatial 4-SPU and 1-UPU parallel manipulator with 5-driving limbs is designed, as shown in Fig. 9a. It includes a pentagonal moving platform m, a pentagonal base B, one extendable UPU driving limb with a hydraulic cylinder and a piston-rod, and four extendable SPU driving limbs with their hydraulic cylinders and piston-rods. Where, m is an equilateral quadrangle $(a_1a_2a_3a_4)$ with a_0 as its center, and B is an equilateral quadrangle plane $(A_1A_2A_3A_4)$ with A_0 as its center. Four identical SPU driving limbs connect m to B by a spherical joint S at point a_i, a driving limb r_i with a prismatic joint P, and a universal joint U at point A_i $(i = 1, 2, 3, 4)$, respectively. 1-UPU driving limb connects m to B by a universal joint U at point a_0 a driving limb r_5 with a prismatic joint P, and a universal joint U at point A_0.

By inspecting this whole mechanism, we know that $k = 12$ for one moving platform, five cylinders, and five piston-rods, and one base; $j = 15$ for six universal joints U, five prismatic joints P, and four sphere joints S; $f_1 = 2$ for the universal joint, $f_2 = 1$ for the prismatic joint, $f_3 = 3$ for the sphere joint; $F_0 = 0$. Therefore, based on Eq. (1), the DOF of the whole mechanism is

$$F = \lambda(k - j - 1) + \sum_{i=1}^{n} f_i - F_0 = 6 \times (12 - 15 - 1) + (6 \times 2 + 5 \times 1 + 4 \times 3) - 0 = 5 \qquad (5)$$

A simulation mechanism of the spatial 4-SPU and 1-UPU parallel manipulator is created in the 3D sketch environment, as shown in Fig. 9b. Its creation processes are described as follows.

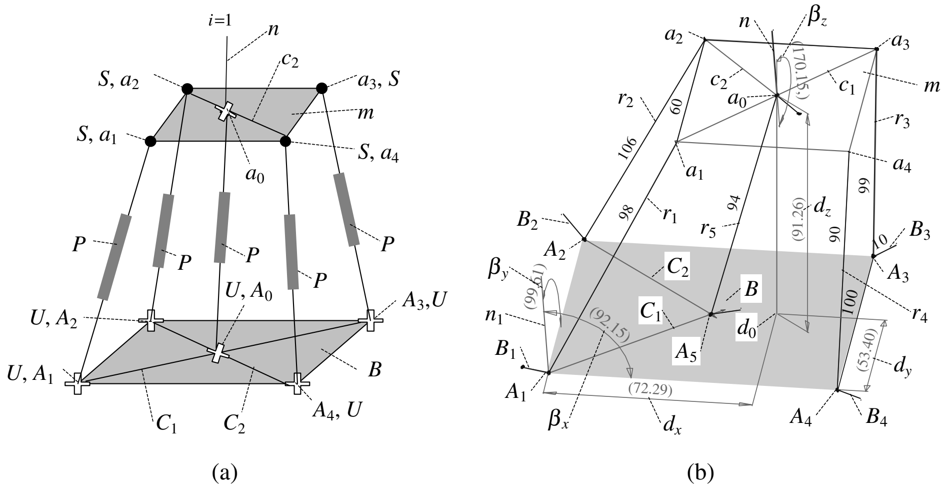

Fig. 9. (a)The spatial 4-SPU and 1-UPU parallel manipulator and (b) its simulation mechanism. The 4-SPU and 1-UPU parallel manipulator with 5-driving limbs and its simulation mechanism.

1. Follow the step 2 in the common technique, constitute a moving platform ($a_1a_2a_3a_4$) with sideline (60 cm) in length, and a base ($A_1A_2A_3A_4$) with sideline (100 cm) in length, respectively.
2. Follow the steps 6 and 7 in the common technique, constitute four equivalent SPU driving limbs (r_1, r_2, r_3 and r_4) and one equivalent UPU driving limb r_5, respectively. In this way, a simulation mechanism of the spatial 4-SPU and 1-UPU parallel manipulator is created.
3. The position-orientation of the moving platform of the spatial 4-SPU and 1-UPU parallel manipulator can be determined by adopting similar processes in Section 3.2.

5.2. The 4-PSU and 1-UPU parallel manipulator and its simulation mechanism

A new type of spatial 4-PSU and 1-UPU parallel manipulator with 5-driving limbs is designed, as shown in Fig. 10a. It includes a moving platform m, a base B, 1-UPU driving limb, and 4-PSU driving limbs. Where, m is an equilateral quadrangle ($a_1a_2a_2a_4$) with a_0 as its center. B is cubic frame, in which an equilateral quadrangle plane ($A_1A_2A_2A_4$) is connected onto another equilateral quadrangle plane ($B_1B_2B_2B_4$) by the four vertical columns A_iB_i $(i = 1, 2, 3, 4)$, respectively. The four prismatic joints P_i are retained coincident with the four vertical columns A_iB_i $(i = 1, 2, 3, 4)$, respectively.

By inspecting the whole mechanism, we know that $k = 12$ for one moving platform, five cylinders, and five piston-rods, and one base; $j = 15$ for six universal joints U, five prismatic joints P, and four sphere joints S; $f_1 = 2$ for the universal joint, $f_2 = 1$ for the prismatic joint, $f_3 = 3$ for the sphere joint; $F_0 = 0$. Therefore, based on Eq. (1), the DOF of the whole mechanism is

$$F = \lambda(k - j - 1) + \sum_{i=1}^{n} f_i - F_0 = 6 \times (12 - 15 - 1) + (6 \times 2 + 5 \times 1 + 4 \times 3) - 0 = 5 \qquad (6)$$

A simulation mechanism of the spatial 4-PSU and 1-UPU parallel manipulator is created in the 3D sketch environment as shown in Fig. 10b, and its creation processes are described below.

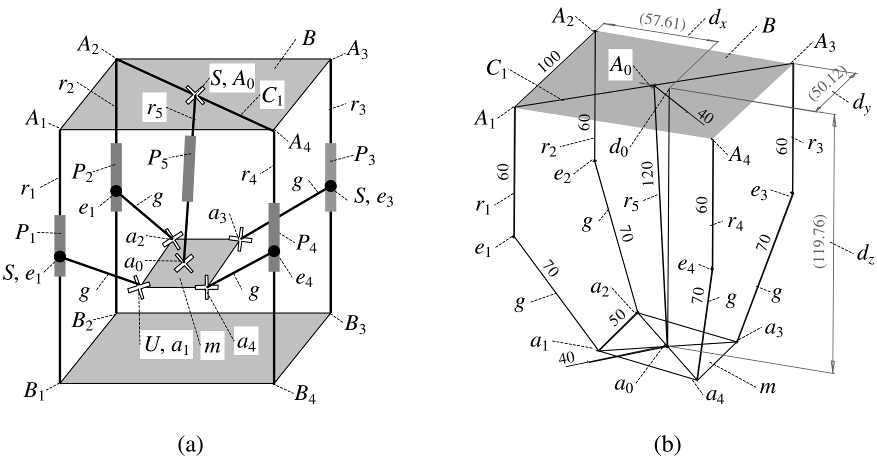

Fig. 10. (a) The spatial 4-PSU and 1-UPU parallel manipulator and (b) its simulation mechanism. The 4-PSU and 1-UPU parallel manipulator with five DOF and its simulation mechanism.

1. Follow the step 2 in the common technique, constitute a moving platform ($a_1a_2a_3a_4$) with sideline (50 cm) in length, and a base plane ($A_1A_2A_3A_4$) with sideline (100 cm) in length, respectively.
2. Constitute four lines A_ie_i, connect their one ends to point A_i $(i = 1, 2, 3, 4)$ of the base plane ($A_1A_2A_3A_4$), respectively, by using the point–point coincident command, and set A_ie_i perpendicular to the base plane.
3. Follow the steps 3e, 6, and 7 in the common technique, constitute four equivalent PSU driving limbs (r_1, r_2, r_3 and r_4) and an equivalent UPU driving limb r_5, respectively. In this way, a simulation mechanism of the 4-PSU and 1-UPU spatial parallel manipulator is created.
4. The position-orientation of the moving platform of the 4-PSU and 1-UPU spatial parallel manipulator can be determined by adopting similar processes in Section 3.2.

6. Spatial parallel manipulator with 6-driving limbs

6.1. The 3/6-SPS parallel manipulator and its simulation mechanism

An existing Stewart 3/6-SPS spatial parallel manipulator has six DOF [1,13,14]. It includes a moving platform m, a base B, and six extendable driving limbs r_i with their hydraulic cylinders and piston-rods, as shown in Fig. 11a. The moving platform is a regular triangle $\Delta a_1a_2a_3$ with a_0 as its center. The base is a regular hexagon ($A_1A_2A_3A_4A_5A_6$) with A_0 as its center. Six identical SPS driving limbs r_i connect m to B by a spherical joint S at point $a_k(k = 1, 2, 3)$, a driving limb r_i with a prismatic joint P, and a spherical joint S at point A_i $(i = 1, 2, \dots, 6)$, respectively.

A simulation mechanism of the spatial 3/6-SPS parallel manipulator is created as shown in Fig. 11b. The creation processes are explained as follows.

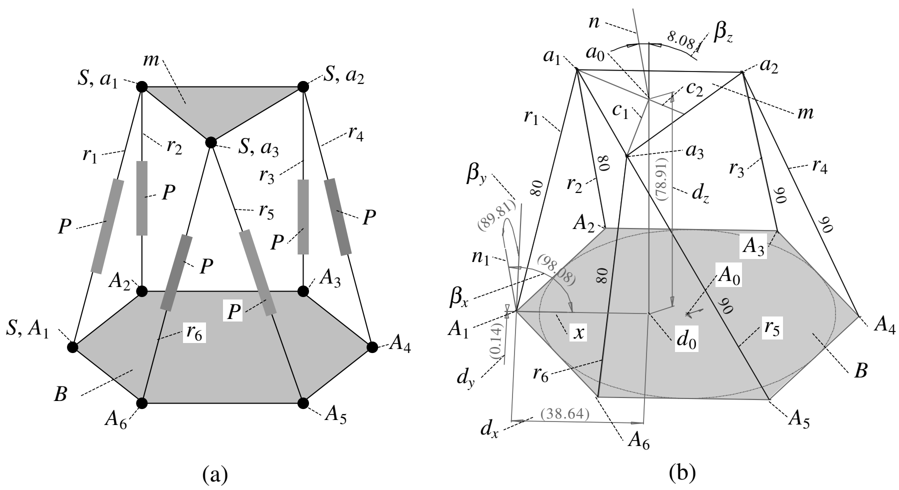

Fig. 11. (a) The 3/6-SPS parallel manipulator and (b) its simulation mechanism. The 3/6-SPS parallel manipulator and its simulation mechanism.

1. Follow the step 2 in the common technique, constitute an equilateral hexagon plane ($A_1A_2A_3A_4A_5A_6$) with sideline (50 cm) in length, and take it as the base. Constitute an equilateral triangle $\Delta a_1a_2a_3$ with sideline (50 cm) in length, and take it as the moving platform.
2. Follow the step 5 in the common technique, constitute 6-SPS driving limbs r_i $(t = 1, 2, \ldots, 6)$ and give each driving limb an initial driving dimension (90 cm) in length. In this way, a simulation mechanism of the 3/6-SPS parallel manipulator is created.
3. The position-orientation of the moving platform of the 3/6-SPS simulation mechanism can be determined by adopting similar processes in Section 3.2.

By inspecting this whole mechanism, we know that $k = 14$ for one moving platform, six cylinders, and six piston-rods, and one base; $j = 18$ for six prismatic joints P, six sphere joints S on B, and six sphere joints S on M which are transformed into three composite sphere joints S; $f_1 = 1$ for the prismatic joint, $f_2 = 3$ for the sphere joint; $F_0 = 6$ for 6-driving limb rotating about themselves axis. Therefore, based on Eq. (1), the DOF of the whole mechanism is

$$F = \lambda(k - j - 1) + \sum_{i=1}^{n} f_i - F_0 = 6 \times (14 - 18 - 1) + (6 \times 1 + 12 \times 3) - 6 = 6 \quad (7)$$

6.2. The 6-SPS spatial parallel manipulator and its simulation mechanism

An existing Stewart–Gough 6-SPS spatial parallel manipulator has six DOF [1,13,14]. It includes a moving platform m, a base B, and six extendable driving limbs r_i with the hydraulic cylinder and the piston-rod, as shown in Fig. 12a. Where, m is a regular hexagon ($a_1a_2a_3a_4a_5a_6$) with a_0 as its center, and B is the regular hexagon ($A_1A_2A_3A_4A_5A_6$) with A_0 as its center. Six identical SPS driving limbs r_i connect m to B by a spherical joint S at point a_i, a driving limb r_i with a prismatic joint P, and a spherical joint S at point A_i $(i = 1, 2, \ldots, 6)$, respectively.

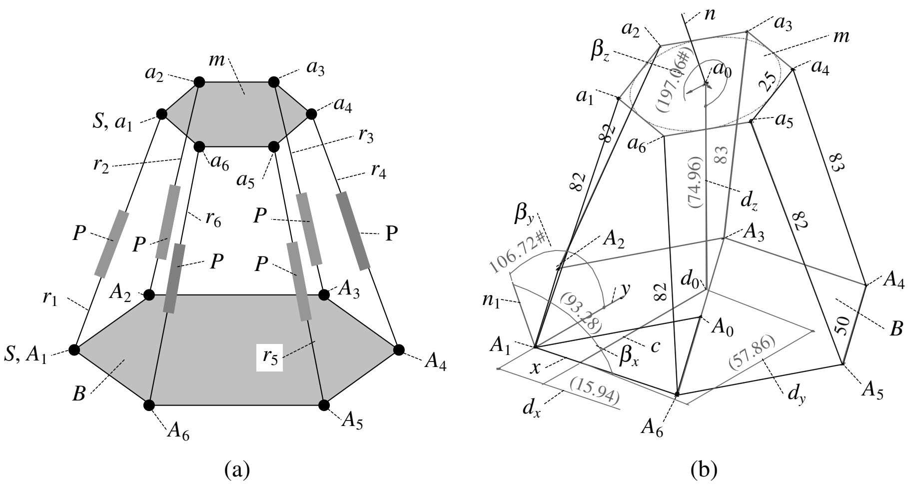

Fig. 12. (a) The 6-SPS parallel manipulator and (b) its simulation mechanism. The Stewart–Gough 6-SPS parallel manipulator and its simulation mechanism.

By inspecting this whole mechanism, we know that $k = 14$ for one moving platform, six cylinders, and six piston-rods, and one base; $j = 18$ for six prismatic joints P, six sphere joints S on B, and six sphere joints S on M; $f_1 = 1$ for the prismatic joint, $f_2 = 3$ for the sphere joint; $F_0 = 6$. Therefore, the DOF of the whole mechanism is the same as that of Stewart 3/6-SPS spatial parallel manipulator.

A simulation mechanism of the 6-SPS spatial parallel manipulator with 6-driving limbs is created, as shown in Fig. 12b. The creation processes are explained as follows.

1. Follow the step 2 in the common technique, constitute an equilateral hexagon $(A_1A_2A_3A_4A_5A_6)$ with sideline (50 cm) in length, and take it as the base. Constitute an equilateral hexagon plane $(a_1a_2a_3a_4a_5a_6)$ with sideline (25 cm) in length, and take it as the moving platform.
2. Follow the step 5 in the common technique, constitute 6-SPS driving limbs r_i $(i = 1, 2, \ldots, 6)$ and give each driving limb an initial driving dimension (82 cm) in length. In this way, a simulation mechanism of the 6-SPS parallel manipulator with 6-driving limbs is created.
3. The position-orientation of the moving platform of the 6-SPS simulation mechanism can be determined by adopting similar processes in Section 3.2.

6.3. The 6-SSP spatial parallel manipulator and its simulation mechanism

A new type of the 6-SSP spatial parallel manipulator is designed, as shown in Fig. 13a. It includes a moving platform m, a base B, six binary links, and six extendable driving limbs r_i with the hydraulic cylinder and the piston-rod. Where, m is a regular hexagon $(a_1a_2a_3a_4a_5a_6)$ with a_0 as its center, and B is an equilateral quadrangle link $(B_1B_3B_4B_6)$ with three translation paths. Six identical SSP driving limbs connect m to B by a spherical joint S at point a_i, binary link g_i, a

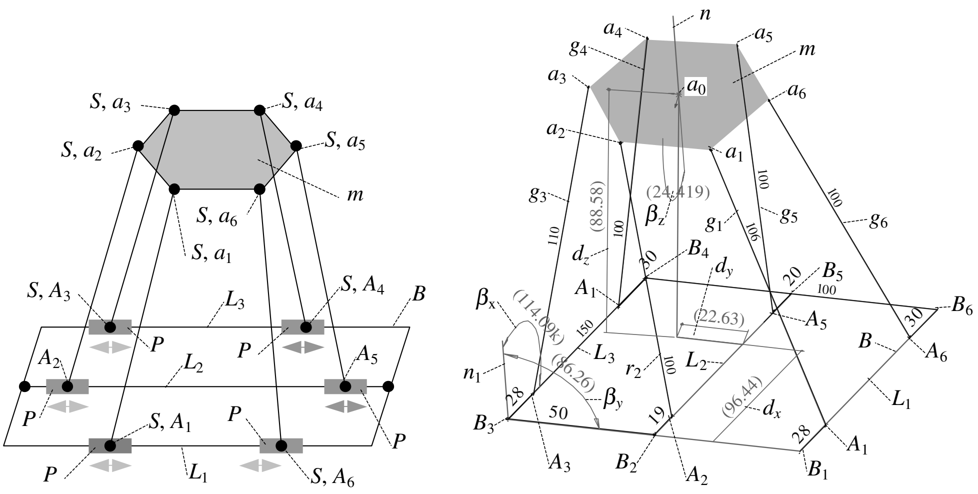

(a) (b)

Fig. 13. (a) The 6-SSP parallel manipulator and (b) its simulation mechanism. The 6-SSP parallel manipulator and its simulation mechanism.

spherical joint S at point A_i, and a driving limb r_i with a prismatic joint P at point A_i, $i = 1, 2, \ldots, 6$), respectively.

By inspecting the whole mechanism of Fig. 13a, we know that $k = 14$ for the six cylinders, six piston-rods, one base, and one moving platform; $j = 18$ for the 12 spherical joints S, and six prismatic joints P; $f_1 = 3$ for spherical joint, $f_2 = 1$ for prismatic joints; $F_0 = 6$ for the six binary links rotating about their axis. Therefore, the DOF of the 6-SSP parallel manipulator is determined as follows.

$$F = \lambda(k - j - 1) + \sum_{i=1}^{n} f_i - F_0 = 6 \times (14 - 18 - 1) + (12 \times 3 + 6 \times 1) - 6 = 6 \quad (8)$$

A simulation mechanism of the spatial 6-SSP parallel manipulator with 6-driving limbs is created as shown in Fig. 13b. The creation processes are explained as follows.

1. Follow the step 2b in the common technique, constitute an equilateral hexagon plane ($a_1a_2a_3a_4a_5a_6$) with sideline (50 cm) in length, and take it as the moving platform.
2. Follow the step 2d in the common technique, constitute an equilateral quadrangle link ($B_1B_3B_4B_6$) with sideline (100 cm) in length, and take it as the base. Constitute a line L_2 and connect its two ends to the middle point B_2 of sideline B_1B_3 and the middle point B_5 of sideline B_4B_6, respectively, by using the point–line coincident command.
3. Follow the steps 3e and 7 in the common technique, constitute six lines g_i, ($i = 1, 2 \ldots, 6$), give each of them an initial fixed dimension (100 cm) in length. Connect their two ends to the moving platform at point a_i and the base at point A_i, respectively. Thus, 6-SSP driving limbs are constituted. In this way, a simulation mechanism of the spatial 6-SSP parallel manipulator with 6-driving limbs is created.
4. The position-orientation of the moving platform of the 6-SSP simulation mechanism can be determined by adopting similar processes in Section 3.2.

6.4. The spatial 6-SPRP parallel manipulator and its simulation mechanism

From the spatial 3-SRP parallel manipulator of Fig. 6a, replace the three binary links g_i by the extendable driving limbs r_i with the hydraulic cylinder and the piston-rod ($i = 1, 2, 3$), respectively. In this way, a new type of the spatial 6-SPRP parallel manipulator is designed. It includes a moving platform m, a base B, and six extendable driving limbs with their hydraulic cylinders and piston-rods, as shown in Fig. 14a. Moreover, this mechanism is partially parallel and partially serial, which is often referred to as hybrid structure.

By inspecting the whole mechanism of Fig. 14, we know that $k = 11$ for the six cylinders, three piston-rods, one base, and one moving platform; $j = 12$ for the three spherical joints S, and six prismatic joints P, three revolute joints R; $f_1 = 3$ for spherical joint, $f_2 = 1$ for prismatic joints, $f_3 = 1$ for revolute joints; $F_0 = 0$. Therefore, the DOF of the 6-SSP parallel manipulator is

$$F = \lambda(k - j - 1) + \sum_{i=1}^{n} f_i - F_0 = 6 \times (11 - 12 - 1) + (3 \times 3 + 6 \times 1 + 3) - 0 = 6 \quad (9)$$

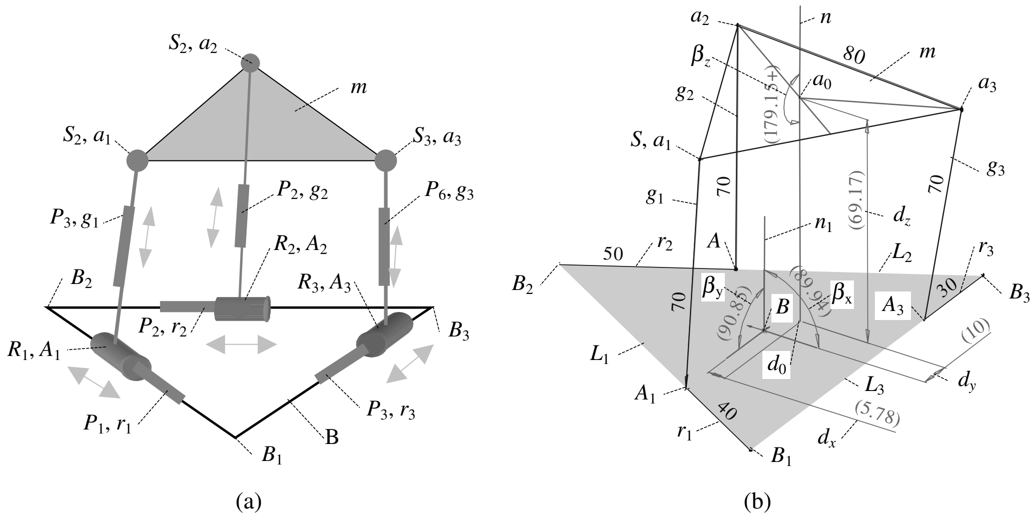

Fig. 14. (a) The 6-SPRP parallel manipulator and (b) its simulation mechanism. The 6-SPRP parallel manipulator and its simulation mechanism.

A simulation mechanism of the spatial 6-SPRP parallel manipulator with 6-driving limbs, as shown in Fig. 14b is similar to that of spatial 3-SRP parallel manipulator, as shown in Fig. 6b, except that the fixed dimension of the three binary links g_i $(i = 1, 2, 3)$ are transformed into driving dimension.

7. Solving displacement of the moving platform

In the light of the simulation mechanism of the spatial 3-UPU parallel manipulator as shown in Fig. 4b, when set $l_i = 50$ cm, $L_i = 120$ cm $(i = 1, 2, 3)$, its original configuration is changed into a new one as shown in Fig. 14a. Therefore, once a simulation mechanism is created, it can be used repeatedly for synthesizing same type of spatial parallel mechanism with different sizes and configurations. The three position components of the moving platform of the 3-UPU simulation mechanism can be solved, and the solving processes are explained below.

In the environment of the 3-UPU simulation mechanism, a data sheet of Microsoft Excel is embedded into the sketching interface of the CAD software. Next, click each driving dimension of driving limbs, thus their dimension names (r_1, r_2 and r_3) are automatically listed in the first row of the data sheet. After that, fill the three driving dimensions (r_1, r_2 and r_3) from 80 to 120 cm with different increments (1, 1.5 and 2) and the number of configurations into their corresponding column, respectively, by using automatically filling function. Thus, the 20 different configurations of the simulation mechanism are constituted. Each configuration corresponds to each row driving dimensions of (r_1, r_2 and r_3). When any one of all configurations is active, the 3-UPU simulation mechanism will be varied and can be directly visualized on screen. Thus the position components of the moving platform of spatial 3-UPU parallel manipulator can be solved automatically. The

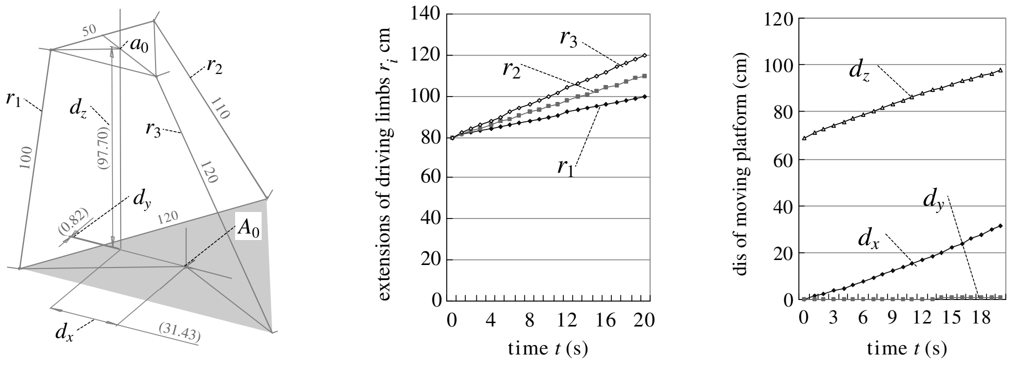

(a) (b) (c)

Fig. 15. (a) 3-UPU simulation mechanism; (b) driving dimension of driving limbs and (c) position components. The three position components of the spatial 3-UPU parallel manipulator.

simulation results of position components of the spatial 3-UPU parallel manipulator are retained the same as that of analytics' approach, as shown in Fig. 15.

8. Conclusions

By applying the computer aided geometry constraint and dimension driving techniques in 3D sketch environment of the advanced CAD software, the simulation mechanisms of the some new and original spatial parallel manipulators with 3-, 4-, 5-, 6-driving limbs can be designed. When modifying the driving dimensions of driving limbs by using the dimension driving technique, the configurations of the simulation mechanisms are varied correspondingly. In this way, the kinematic parameters of the moving platform of each simulation mechanism can be solved.

When all the driving dimensions and the fixed dimensions of simulation mechanism are modified, all the geometric constraints and dimension constraints in each simulation mechanism are always retained. Therefore, once a simulation mechanism is created, it can be used repeatedly for synthesizing same type of spatial parallel mechanism with different sizes and configurations.

When modifying the driving dimension in simulation mechanism, the driven dimension will be varied correspondingly. In this way, based on the DOF of parallel spatial mechanism, the number of driving dimensions of the simulation mechanism can be determined.

By applying the driving and driven dimension technique and recording function, the position-orientation of the moving platform in respect to the base can be solved. The approximate velocity (and rotation speed) and the approximate acceleration (and rotational acceleration) of the moving platform in respect to the base can be solved by using the fit curve and the fit equation technique in Microsoft Excel environment.

The simulation results prove that the computer aided geometric approach is equivalent to the analytical for tasks of structure synthesis and kinematic analysis, and is not only fairly quick, straightforward, but also advantages from viewpoint of accuracy and repeatability.

References

[1] D. Stewart, A platform with six degrees of freedom, Proc. Inst. Mech. Eng. Part I 180 (15) (1965) 371–386.

[2] K.H. Hunt, Structural kinematics of in-parallel actuated robot arms, Trans. ASME J. Mech. Trans. Automat. Des. 105 (4) (1983) 705–712.

[3] Z. Huang, Q. Li, Type synthesis principle of minor-mobility parallel manipulators, Sci. China (Ser. E) 45 (3) (2002) 241–248.

[4] L.W. Tsai, F. Tahmasebi, Synthesis and analysis of a new class of six-degree of freedom parallel minimanipulators, J. Robot. Syst. 10 (5) (1993) 561–580.

[5] F. Gao, W. Li, X. Zhao, New kinematic structures for 2-,3-,4- and 5-DOF parallel manipulator designs, Mech. Mach. Theory 37 (2002) 1395–1411.

[6] L.W. Tsai, S. Joshi, Kinematics and optimization of a spatial 3-UPU parallel manipulator, Trans. ASME J. Mech. Des. 122 (4) (2000) 439–446.

[7] Z. Huang, Y.F. Fang, Kinematic characteristics analysis of 3-DOF in-parallel actuated pyramid mechanisms, Mach. Mech. Theory 31 (8) (1996) 1009–1018.

[8] Z. Huang, J. Wang, Identification of principal screws of 3-DOF parallel manipulators by quadric degeneration, J. Mech. Mach. Theory 36 (8) (2001) 893–911.

[9] C.M. Gosselin, On the direct kinematics of spherical 3-DOF parallel manipulators, Int. J. Robot. Res. 12 (4) (1993) 394–402.

[10] C.M. Gosselin, J. Angeles, The optimum kinematic design of a spherical 3-DOF parallel manipulator, Trans. ASME J. Mech., Transm., Autom. 116 (4) (1994) 1141–1147.

[11] H.Y. Lee, B. Roth, A closed-form solution of the forward displacement analysis of a class of in-parallel mechanisms, in: Proceedings of IEEE International Conference on Robotics Autumatiom, 1993, pp. 720–724.

[12] S.V. Sreentvasan, K.J. Waldron, Closed-form direct displacement analysis of 6–6 Stewart platform, J. Mech. Mach. Theory 29 (2) (1994) 855–864.

[13] B. Dasgupta, T.S. Mruthyunjaya, A constructive predictor–corrector algorithm for the direct position kinematic problem for a general 6–6 Stewart platform, J. Mech. Mach. Theory 31 (6) (1996) 799–811.

[14] R.I. Alizade, N.R. Tagiyev, J. Duffy, A forward and reverse displacement analysis of a 6-DOF in-parallel manipulators, J. Mech. Mach. Theory 29 (1) (1994) 115–124.

[15] K. Luck, Computer-aided mechanism synthesis based on the Burmester theory, J. Mech. Mach. Theory 29 (6) (1994) 877–886.

[16] R. Matone, B. Roth, In-parallel manipulators: a framework on how to model actuation schemes and a study of their effects on singular postures, Trans. ASME, J. Mech. Des. 121 (1) (1999) 2–8.

[17] P.N. Sheth, A digital computer based simulation procedure for multiple degree of freedom mechanical systems with geometric constraints, Doctoral dissertation, University of Wisconsin, 1972, University Microfilm no.73–2565.

[18] C.M. Gosselin, L. Pereault, Ch. Vaillancourt, Simulation and computer-aided kinematic design of three-degree-of freedom spherical parallel manipulators, J. Robot. Syst. 12 (12) (1995) 857–869.

[19] T.J. Furlong, J.M. Vance, P.M. Larochelle, Spherical mechanism synthesis in virtual reality, Trans. ASME, J. Mech. Des. 121 (4) (1999) 515–520.

[20] Y.M. Deng, G.A. Britton, S.B. Tor, Constraint-based functional design verification for conceptual design, Comput.-Aided Des. 32 (14) (2000) 889–899.

[21] Q.J. Ge, M. Sirchia, Computer aided geometric design of two parameters free form motion, Trans. ASME, J. Mech. Des. 121 (4) (1999) 9–14.

[22] Y. Lu, T. Leinonen, Computer aided geometric approach of approximate dimensional synthesis with four-bar linkage, J. Comput. Aided Des. Graph. 14 (6) (2002) 547–552.

[23] Y. Lu, T. Leinonen, Computer Simulation mechanism approach for higher-order and combined point-order approximation synthesis, J. Comput. Aided Des. Graph. 14 (8) (2002) 845–851.

[24] Y. Lu, T. Leinonen, Computer simulation approach of manufacturing complicated shape on orthogonal 6-rod virtual machine tool, Int. J. Mach. Tool Manuf. 42 (3) (2002) 441–447.

[25] Y. Lu, Computer simulation of manufacturing 3-D free surface on orthogonal 3-rod virtual machine tool, Int. J. Mach. Tool Manuf. 43 (11) (2002) 734–742.